Polym. Bull. (2011) 67:985–995
DOI 10.1007/s00289-010-0440-5

ORIGINAL PAPER

Synthesis and characterization of thermosensitive core–shell polymeric nanoparticles

I. A. Facundo · M. J. Soria · M. G. Rosales · L. E. Elizalde · R. Díaz de León · H. Saade · R. G. López

Received: 8 September 2010 / Revised: 21 December 2010 / Accepted: 30 December 2010 /
Published online: 21 January 2011

Abstract Thermosensitive core–shell nanoparticles were synthesized by semicontinuous heterophase polymerization of styrene, followed by a seeded polymerization for forming a shell of poly(*N*-isopropyl acrylamide) (PNIPAM). Nanoparticles characterization by scanning transmission electronic microscopy showed core–shell morphology with average particle diameters around 40 nm. An inverse dependence of the particle size with temperature in the range 20–55 °C was identified by quasielastic light scattering measurements. As was expected for core–shell particles with PNIPAM as the shell, a volume phase transition near 32 °C was detected. In spite of thermosensitive properties of core–shell nanoparticles synthesized here, the volume percentage loss values were not so high, probably due to their relatively low content of PNIPAM.

Keywords Thermosensitive nanoparticles · Core–shell · Semicontinuous heterophase polymerization

Introduction

Research on the synthesis and characterization of thermosensitive polymeric particles has received increasing attention in the last years, because of their unique properties [1–4]. Thermosensitive core–shell polymeric particles usually consist of a core of polystyrene (PS) and a shell of a polymer of acrylamide derivatives [4]. In water

I. A. Facundo · M. J. Soria · M. G. Rosales
Facultad de Metalurgia, UA de C, Carretera 57 km.5, Monclova, Coahuila 25710, Mexico

L. E. Elizalde · R. D. de León · H. Saade · R. G. López (✉)
Centro de Investigación en Química Aplicada, Blvd. Ing. Enrique Reyna No. 140,
Saltillo, Coahuila 25253, Mexico
e-mail: glopez@ciqa.mx

L. E. Elizalde
e-mail: elizalde@ciqa.mx

dispersion at temperatures below the lower critical solution temperature (LCST), water swells the thermosensitive shell. At temperatures higher than LCST the shell shrinks, releasing water molecules and leading to a decrease in the particle size. This property has been used as a basis for the development of a number of applications in biology [5–7]. Another interesting application of this type of particles is in the development of catalytic systems [8–11]. In these systems metallic nanoparticles acting as catalysts are embedded into the shell. Once the core–shell particles are suspended in water, at temperatures < LCST the reagents can diffuse to the metallic nanoparticles for carrying out reactions. When the temperature is increased above LCST the polymer network in the shell shrinks, leading to a decrease in the catalytic activity.

One interesting point of the thermosensitive particles is the response time to a temperature change. Concerning this, Tanaka et al. [12] reported that the response time is proportional to the square of the particle radius. This characteristic is important because the use of very small thermosensitive core–shell particles would allow a reduction in the response time in those applications in which a sharp response is desirable.

Despite their potential applications, a detailed search in the specialized literature showed a total absence of reports about the preparation of thermosensitive core–shell polymeric nanoparticles. The synthesis of the smallest particles of this type reported in the literature, with an average particle diameter ranging from hundreds of nanometers to micrometers, usually includes a surfactant-free emulsion polymerization for obtaining a PS core. After that, a seeded polymerization is carried out for forming the shell of a crosslinked polymer of an acrylamide derivative, such as poly(*N*-isopropyl acrylamide) (PNIPAM) [13–18]. The synthesis of very small thermosensitive core–shell polymeric particles can be achieved starting with the preparation of the core by semicontinuous heterophase polymerization. Similar to batch microemulsion polymerization, this technique is capable of producing polymeric nanoparticles of 20–50 nm in average diameter [19–21]. However, the surfactant concentrations are much lower than those used in batch microemulsion polymerization. In order to form the shell, a seeded polymerization must be carried out by adding an acrylamide derivative monomer on a core aqueous dispersion.

Here we report the synthesis of thermosensitive core–shell nanoparticles with an average particle diameter in a non-swollen state around 40 nm. The process includes the preparation of a PS core by semicontinuous heterophase polymerization at 60 °C followed by a seeded emulsion polymerization at 70 °C for forming the PNIPAM shell. This temperature is above the LCST of PNIPAM, that is, 31–32 °C [17, 18]. The particle size and thermosensitive behavior of the obtained particles were determined. As far as we know, this is the first report on the synthesis of thermosensitive PS–PNIPAM core–shell nanoparticles with an average diameter <50 nm in a non-swollen state.

Experimental section

Materials

All chemicals were reagent-grade. Styrene (St) (99%) from Sigma-Aldrich was distilled under reduced pressure and stored at 4 °C. Potassium persulfate (KPS)

(99.99%), sodium dodecyl sulfate (SDS) (98%), NIPAM (97%) and *N*,*N*′-methylene bisacrylamide (MBA) (99.00%), all of them from Sigma-Aldrich and sodium bis (2-ethylhexil) sulfosuccinate (AOT) from Fluka were used as received. De-ionized and triple-distilled water was drawn from a Millipore system.

Synthesis of PS core

The recipe and the procedure used for the synthesis of the PS core were established on the basis of previous experimentation performed by our group [22]. The polymerization was carried out at 60 °C in a 150 mL jacketed glass reactor equipped with a reflux condenser and inlets for argon, monomer feed, mechanical agitation (450 rpm) and sampling. A 45°-pitched down flow four-bladed impeller was used. The procedure was as follows: 3.36 g of SDS, 1.13 g of AOT, and 0.06 g of KPS were dissolved in 96.03 g of water and charged into the reactor. The mixture SDS/AOT (3/1, w/w) used here was chosen because it gives great stability to polymeric particles as has been demonstrated by our group in batch [23] and semicontinuous [20, 24, 25] polymerizations. This solution was bubbled with argon for 1 h and then heated to 60 °C. After that, 34.56 g of St was fed at a rate of 0.072 g/min using a KD Scientific syringe pump. After the addition of the monomer was completed (8 h), the reaction was allowed to proceed for one more hour. Samples were withdrawn at given times to determine conversions by gravimeter. Instantaneous (x_i) and global (X) conversions were determined along the polymerization. The instantaneous conversion is the fraction of added monomer up to time t that has changed into polymer whereas the global conversion is the fraction of total monomer added in the process that has reacted into polymer at time t. For knowing the monomer and polymer concentrations in the reaction mixture along the polymerization, a mass balance was made each time a sample was taken. For this, the weight of the added monomer up to the sampling time, and those of the taken sample and of the polymer in the sample were used.

Synthesis of core–shell nanoparticles

The recipe and the procedure used for the synthesis of the core–shell nanoparticles were established on the basis of previous experimentation performed by our group [22]. This reaction was carried out in a 100 mL jacketed glass reactor with an experimental arrangement similar to the system in which PS core was obtained. Shell of PNIPAM was formed onto the PS core by a seeded polymerization described as follows. 22.5 g of the previously prepared PS latex were charged into the reactor and bubbled with argon for 1 h. After that, the mixture was heated to 70 °C, the required amount of KPS (2 wt% with respect to NIPAM) dissolved in 1.9 g of water was added, and the dosing of 26.1 g of an aqueous solution of NIPAM and MBA was started at a dosing rate of 0.11 g/min and maintained for 4 h. Once the addition was finished, the polymerization was allowed to proceed for six more hours. Two seeded polymerizations with different ratios PS/NIPAM were carried out. The particles core–shell NC1 were prepared using 1.7 g of NIPAM,

while 2.1 g of this acrylamide derivative was used for preparing particles NC2. In both cases 2 wt% of MBA with respect to NIPAM was used as crosslinking agent.

Characterization

Particle sizes were measured in a Malvern Zetasizer Nano S90 Quasielastic Light Scattering (QLS) apparatus equipped with an Argon laser ($\lambda = 633$ nm). The measurements were carried out at 25 °C for the latex sample obtained at the end of St polymerization and at different temperatures in the range 20–50 °C for those latex samples from the end of core–shell polymerizations. Before measurements, latex samples were diluted with water up to 200 times. Intensity correlation data were analyzed by the method of cumulants to provide the average decay rate $\langle\Gamma\rangle$ ($= 2q^2D$, where D is the diffusion coefficient and q is the modulus of the scattering vector). The measured diffusion coefficients were used to calculate the apparent diameters by means of the Stokes–Einstein relation with the assumption that the continuous phase has the viscosity of water. The so-obtained diameter is the intensity-weighted average diameter (D_z). Particle size and polydispersity index (PDI) were also determined in a JEOL JSM-7401F scanning-transmission electron microscope (STEM). For this, 0.01 g of latex was diluted in 10 g of water, and a drop of this dispersion was added to a copper grid, and allowed to dry. At least 500 particles were measured from the micrographs to obtain the PDI (D_w/D_n), being D_w and D_n the weight- and number-average diameters, respectively, which were calculated using the following equations:

$$D_n = \frac{\sum_i n_i D_i}{\sum_i n_i} = \frac{\sum n_i D_i}{n} \tag{1}$$

$$D_w = \frac{\sum_i n_i D_i^4}{\sum_i n_i D_i^3}, \tag{2}$$

where n_i is the number of particles of size D_i and n is the total number of measured particles.

Results and discussion

Figure 1 shows the evolution of the instantaneous (x_i) and global (X) conversions with the polymerization time (t). This figure reveals that x_i increases rapidly and reaches values close to 70–75% at early stages of the reaction. After that, x_i increases slowly attaining a value of 89% at the end of the addition stage. This behavior indicates that polymerization was carried out at the so called monomer-starved conditions. Krackeler and Naidus [26] introduced this concept for explaining the reduced particle growth and the formation of a large number of polymer particles in the emulsion polymerization of St carried out in semi-continuous mode in comparison to the batch process. These authors invoked the correlation developed for emulsion polymerization by Smith and Ewart [27] for predicting the number of particles (N_P) for the case-II kinetics, in which N_P is

inversely proportional to the volume growth rate of polymer particles during nucleation. In semi-continuous heterophase polymerization during the monomer addition period, when the particles are saturated with monomer, at the so called monomer flooded conditions [28], they grow at their maximum rate. As a consequence the particle nucleation is minimal. In contrast, when monomer concentration in the particles is under the saturation value, that is, at monomer-starved conditions, the particle growth rate slows down and leads to a larger number of smaller particles. In this case, the lower the dosing rate, the lower the monomer concentrations in the particles and the higher x_i. In fact, at highly monomer-starved conditions, x_i values >99% are rapidly achieved and maintained during all the addition period. The evolution of x_i with polymerization time in Fig. 1 suggests that polymerization was carried out at monomer-starved conditions, but not at highly monomer-starved conditions. However, very small nanoparticles of PS were expected.

The measurement by QLS of a latex sample at the end of the polymerization shows a D_z value of 38.2 nm, while the corresponding measurement by STEM gives values for D_n and PDI of 34.0 nm and 1.1, respectively. This very small particle size and the low PDI match with the typical results obtained in a semicontinuous heterophase polymerization carried out at monomer-starved conditions [20, 21]. In accordance with Krackeler and Naidus [26], the monomer dosing rate was sufficiently low for leading to a low monomer concentration in the particles and as consequence, to favor the formation of a large number of small particles.

Previously to the core–shell polymerizations an estimation of the free surfactant in the final latex of PS nanoparticles was carried out. This was very important, because free surfactant promotes the undesirable secondary nucleation during a core–shell polymerization. For knowing this, total particle number (N_P) in the final latex was calculated, using Eq. 3, which was developed from dividing the polymer content by the weight of an average particle:

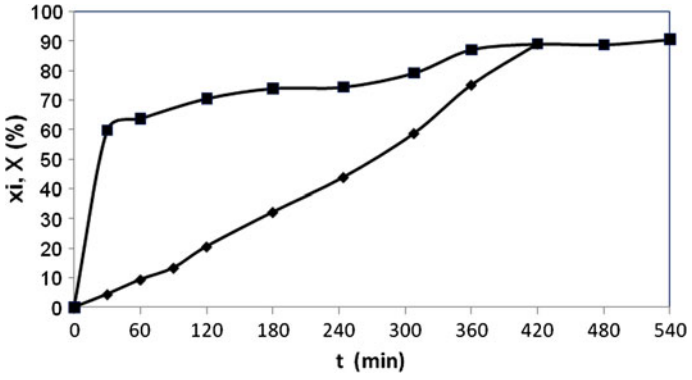

Fig. 1 Instantaneous, x_i (*filled square*) and global conversion, X (*filled diamond*) as a function of time for St polymerization

$$N_P = \frac{C_P}{6\pi\rho_p D_n^3}, \quad (3)$$

where C_P is the polymer content in the latex in g and ρ_p is the PS density, 1.05 g/mL [29]. A total surface area of particles of 5.2×10^{21} nm^2 was obtained by multiplying N_P by the surface area of one particle, calculated from D_n. A value of 4.5×10^{21} nm^2 of total surface coverage by the available surfactant, that is the overall surfactant content less critical micelle concentration (cmc), was obtained by simple calculations, which include the use of a mixing rule based on the molar fractions of the surfactants in the mixture. Critical micelle concentration values of SDS and AOT (7 and 3 mM, respectively) and the values of the molecular surface coverage (a_s), 0.50 and 0.78 nm^2/molecule for SDS and AOT, respectively, were taken from literature [25]. By comparison of the total surface area of particles and the total surface coverage by the available surfactant, is evident that all the surfactant in the PS latex is stabilizing the particles, that is, there is not free surfactant. In fact, as there is not surfactant enough for forming a saturated layer on the particles, is probably that the SO_4^- free radicals attached at the end of the polymer chains are contributing to the stabilization of the particles.

Figure 2 shows the micrographs of PS particles (Fig. 2a) and those of the particles obtained in the core–shell polymerizations (Fig. 2b, c) along with their particle size histograms. The images in Fig. 2b, c suggest a core–shell morphology, with the core represented by the central light area in the spheres and the shell represented by the dark, very thin corona around the central area. Chen et al. [18] reported images for core–shell (PS–PNIPAM) particles similar to ours. However, in

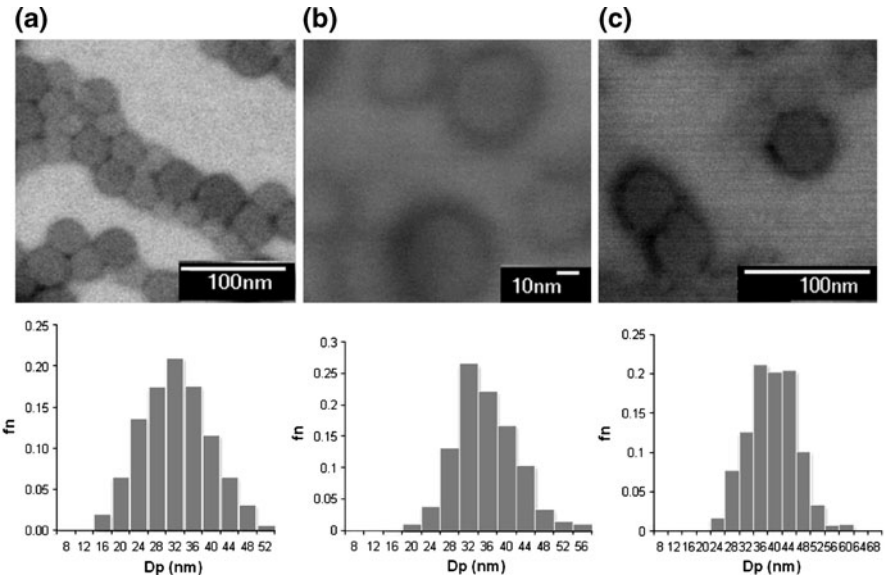

Fig. 2 STEM micrographs and their particle size histograms of: **a** PS seed, **b** NC1 core–shell nanoparticles, and **c** NC2 core–shell nanoparticles

their case, the core is dark and the shell is light, because of the use of transmission electronic microscopy by these authors.

The results of size measurements by QLS and STEM of the particles obtained in the core–shell polymerizations are shown in Table 1. For comparison, the results of size measurements of the previously obtained particles of PS and the expected average diameters of the non-swollen core–shell particles are also included. These latter values were obtained by simple calculations assuming entire polymerization of NIPAM and MBA and the D_n value (from STEM measurement) of the PS particles as the core average diameter. Also, the absence of secondary nucleation and inter-particle coagulation during the core–shell polymerizations were considered. For calculations, the densities of PS and PNIPAM were taken as 1.05 g/mL [29] and 1.12 g/mL [30], respectively. The results in Table 1 show that D_n from STEM measurement and the expected average diameter for particles NC1 are very similar, 37.6 and 37.9 nm, respectively. Furthermore, PDI of PS seed and that of NC1 particles has the same value, that is, 1.1. This suggests that the growth of the seed during core–shell polymerization was exclusively due to the shell formation. In this case, a fraction of the added NIPAM and MBA dissolves in the continuous phase, while the remaining part swelled into the region near the surface of the seed, because they are more hydrophilic than PS. NIPAM and MBA propagate in the continuous phase until they are hydrophobic enough for penetrating into the swollen PS particles, continuing the propagation near their surface for forming a shell of crosslinking PNIPAM [17]. The absence of secondary nucleation is mainly due to that there is not free surfactant in the continuous phase. On the other hand, NC2 particles have a D_n value slightly higher than the expected average diameter (41.3 vs. 38.6 nm) in spite of that their PDI remains equal to that of PS seed with a value of 1.1. This suggests that probably a coagulation process occurred during the polymerization, due to the higher relation NIPAM/PS used in NC2 preparation. However, this process was not intense enough, as indicated by the fact that the value of PDI remained at 1.1. It is noteworthy that the relatively small difference between D_z (38 nm) and D_n (34 nm) for the PS seed becomes considerable when comparing D_z versus D_n in the case of core–shell particles: 50 versus 37.6 nm for NC1 and 54.6 versus 41.3 for NC2. These latter differences arise from the swelling of core–shell particles with water, considering that QLS measurements were carried out at 25 °C, that is, below LCST.

Table 1 Size of seed and core–shell nanoparticles measured by STEM and QLS and those expected from theoretical calculations for core–shell nanoparticles

Particles	STEM		QLS[a]	D_p (nm)
	D_n (nm)	PDI	D_z (nm)	
PS seed	34.0	1.1	38.2	–
NC1	37.6	1.1	50.0	37.9
NC2	41.3	1.1	54.6	38.6

[a] Measured at 25 °C; D_p is the expected average diameter of non-swollen core–shell nano-particles

The change of particle size measured by QLS with temperature for NC1 and NC2 is displayed in Fig. 3. For comparison, the behavior of particle size of PS seed is also included. Table 2 includes the values of D_z for both NC1 and NC2 particles determined at 20 and 55 °C and the volume percentage loss in this temperature interval, as a measure of particle shrinkage because of the expelled water from the particles. Volume percentage loss was calculated using the following equation:

$$\text{Volume\% loss} = (1 - \frac{V_{\text{shrunk}}}{V_{\text{swollen}}})100, \quad (4)$$

where V_{shrunk} and V_{swollen} are the particle volumes calculated from D_z values at 20 and 55 °C, respectively.

It is evident from Fig. 3 and Table 2, that these particles show an inverse dependence of size on temperature, which indicates their thermosensitive character. The decreasing trend of particle size with temperature in Fig. 3 is very clear, while the size of PS particles practically remains the same as temperature increases. The behavior of both of the curves (NC1 and NC2) is similar: the three points in the 20–30 °C interval can be fixed to a straight line (shown in Fig. 3) with a slope 3–5 times that corresponding to the line for the five points in the 35–55 °C interval (shown in Fig. 3). In fact, the intersection of these two straight lines occurs around 31–33 °C, as shown with dotted lines in Fig. 3. This behavior is in accordance with

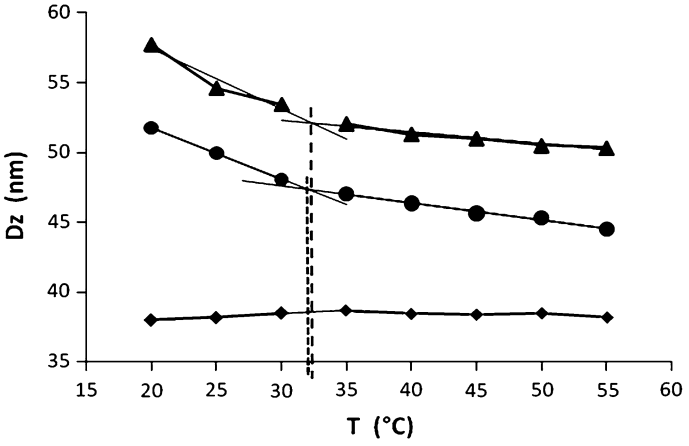

Fig. 3 Change of particle size measured by QLS with temperature for: (*filled diamond*) PS seed, (*filled circle*) NC1 core–shell nanoparticles, and (*filled triangle*) NC2 core–shell nanoparticles. *Dotted lines* indicate the temperature at which a change in the decay trend occurs

Table 2 Size of core–shell nanoparticles at temperatures below and above LCST of NIPAM and the volume percentage loss

Particles	D_z (20 °C) (nm)	D_z (55 °C) (nm)	Volume percentage loss
NC1	51.8	44.5	33
NC2	57.8	50.3	36

that expected for particles with a shell of PNIPAM, because of the LCST value of 31–32 °C reported for PNIPAM [17, 18]. This cannot be a coincidence, taking into account that both of the curves represent the size change with temperature of samples prepared at different core–shell weight ratios using PNIPAM as shell.

In spite of the thermosensitivity of the particles, it is noteworthy that volume loss values (33 and 36% for NC1 and NC2, respectively) are lower than those typically ($\approx$60–95%) reported in the literature for PS–PNIPAM core–shell particles [15, 17, 18]. Furthermore, a somewhat continuous decay trend of particle size with temperature for NC1 and NC2 curves was observed. According to the literature a low volume percentage loss and a somewhat continuous decay trend of particle size with temperature in thermosensitive core–shell particles could be ascribed to a low PNIPAM proportion in the shell and/or a highly crosslinked PNIPAM shell [4]. In our study, NC1 and NC2 particles were prepared with a weight ratio PS/PNIPAM of 78.1/21.9 and 74.1/25.9, respectively, and 2 wt% of MBA with respect to NIPAM as crosslinking agent. Comparatively, Kim and Ballauff [15] studied the preparation of core–shell particles with 40/60 as the PS/PNIPAM weight ratio. For the formation of the shell, they used 6.8% MBA with respect to NIPAM. The particles that they obtained showed a volume percentage loss of 65 in the 10–45 °C interval. Yi and Xu [17] synthesized core–shell particles with a PS/PNIPAM weight ratio of 25.5/74.5 and 1.5 wt% of MBA with respect to NIPAM. These authors reported a volume percentage loss around 96.5% in the temperature interval of 20–50 °C. Chen et al. [18] also reported the synthesis of this type of thermosensitive particles, composed of PS/PNIPAM in a weight ratio of 52.4/47.6, and using 7.9 wt% of MBA with respect to NIPAM. In this case, the volume percentage loss was around 90% in the 10–60 °C interval. From here, it can be observed that the proportion of PNIPAM in the particles NC1 and NC2 are lower than those in the particles prepared in the previously mentioned studies. Regarding the crosslinking agent, the contents used in these studies range from 1.5 to 7.9 wt% with respect to NIPAM. However, even when using the highest content of crosslinking agent (7.9 wt%), a high volume percentage loss was obtained (90%). Comparatively, the content of crosslinking agent used in our study is relatively low. In contrast, it is reported the synthesis of core (PS)–shell (PNIPAM) particles, whose average particle diameters measured by QLS changed from 950 nm at 20 °C to 850 nm at 40 °C [4]. A somewhat continuous decrease of particle size as temperature increased as well as a slight increase in the decay trend in 30–35 °C interval were found. The volume loss was 28%. This low value and the somewhat continuous decrease of particle size versus temperature curve was ascribed by the authors to a partial PNIPAM shell. This was confirmed by the authors when the particles with complete PNIPAM shell showed a change from 1140 to 940 nm in average diameter in the same temperature interval, which equates to a volume loss of 44%. In this case, the curve of particle size versus temperature showed a marked discontinuity around 31–32 °C. Thus, the low volume percentage loss and the somewhat continuous decay trend of particle size with temperature determined for the particles NC1 and NC2 could be due to the low PNIPAM proportion in the particles. In aqueous dispersions of thermosensitive core–shell polymeric particles with PNIPAM shell, at temperatures below LCST, water hydrates the propyl groups of the polymer acrylamide derivative [4]. As a

consequence, a swollen shell is obtained. As the aqueous dispersion temperature increases, water molecules contributing to hydrophobic hydration begin to release from the vicinity of the propyl groups allowing them to form hydrophobic bonds with each other leading to a shrinking of the shell and resulting in a decrease of total particle volume. Below the LCST, this process is rather slow, however, at this temperature it accelerates as a direct function of PNIPAM coverage on the particles [4]. At temperatures higher than LCST, shell continuous to shrink, but much slower.

Conclusions

Semicontinuous heterophase polymerization followed by a seeded polymerization allowed us to obtain PS–PNIPAM core–shell nanoparticles with average diameters around 40 nm and narrow particle size distributions. The increase in the size of the seed and the similar PDI values of the core and the core–shell nanoparticles obtained at the end of the seeded polymerizations, suggests the absence of secondary nucleation, although some coagulation may have occurred. Thus, it is believed that NIPAM polymerized almost exclusively onto the PS cores. Core–shell nanoparticles prepared in this study showed a thermosensitive behavior in the 20–55 °C interval. However, the volume percentage loss values were not so high, probably due to their relatively low content of PNIPAM. This finding could be used as the basis for the development of very small thermosensitive core–shell polymeric nanoparticles with a sharp response time to an appropriate change in temperature. Research on increasing the PNIPAM content in PS–PNIPAM core–shell nanoparticles is ongoing in our group.

Acknowledgments CONACyT supported this research through grants SEP 2003-CO2-45436 and CB-2007-84009. One of us (IAF) acknowledges a scholarship from CONACyT to pursue her doctoral work. We are grateful for Patricia Siller, Daniel Alvarado and José Luis de la Peña for their technical assistance.

References

1. Saunders BR, Vincent B (1999) Microgel particles as model colloids: theory, properties and applications. Adv Colloid Interface Sci 80:1–25
2. Pelton R (2000) Temperature-sensitive aqueous microgels. Adv Colloid Interface Sci 85:1–33
3. Debord JD, Lyon LA (2000) Thermoresponsive photonic crystals. J Phys Chem B 104:6327–6331
4. Kawaguchi B (1999) Thermosensitive hydrogel microspheres. In: Arshady R (ed) Microspheres, microcapsules and liposomes. Citus Books, London, pp 237–252
5. Duracher D, Elaissari A, Mallet F, Pichot C (2000) Adsorption of modified HIV-1 capsid p24 protein onto thermosensitive and cationic core-shell poly(styrene)-poly(*N*-isopropylacrylamide) particles. Langmuir 16:9002–9008
6. Zhang GZ, Wu C (2001) The water/methanol complexation induced reentrant coil-to-globule-to-coil transition of individual homopolymer chains in extremely dilute solution. J Am Chem Soc 123:1376–1380
7. Duracher D, Sauzedde F, Elaissari A, Perrin A, Pichot C (1998) Cationic amino-containing *N*-isopropylacrylamide-styrene copolymer latex particles. Part 1. Particle size and morphology vs. polymerization process. Colloid Polym Sci 276:219–231

8. Lu Y, Mei Y, Drechsler M, Ballauff M (2006) Thermosensitive core-shell particles as carriers for Ag nanoparticles: modulating the catalytic activity by a phase transition in networks. Angew Chem Int Ed 45:813–816
9. Lu Y, Yu M, Drechsler M, Ballauff M (2007) Ag nanocomposite particles: preparation, characterization and application. Macromol Symp 254:97–102
10. Li D, He Q, Li J (2009) Smart core/shell nanocomposites: intelligent polymers modified gold nanoparticles. Adv Colloid Interface Sci 149:23–28
11. Lu Y, Proch S, Schrinner M, Drechsler M, Kempe R, Ballauff M (2009) Thermosensitive core-shell microgel as a nanoreactor for catalytic active metal nanoparticles. J Mater Chem 19:3955–3961
12. Tanaka T, Fillmore DJ (1979) Kinetics of swelling of gels. J Chem Phys 70:1214–1218
13. Makino K, Yamamoto S, Fujimoto K, Kaguaguchi H, Oshima H (1994) Surface structure of latex particles covered with temperature-sensitive hydrogel layers. J Colloid Interface Sci 166:251–258
14. Okubo M, Ahmad H (1996) Adsorption behavior of emulsifiers and biomolecules on temperature-sensitive polymer particles. Colloid Polym Sci 274:112–116
15. Kim JH, Ballauff M (1999) The volume transition in thermosensitive core–shell latex particles containing charged groups. Colloid Polym Sci 277:1210–1218
16. Dingenouts N, Norhausen Ch, Ballauff M (1998) Observation of the volume transition in thermosensitive core–shell latex particles by small-angle X-ray scattering. Macromolecules 31:8912–8917
17. Yi Ch, Xu Z (2005) Synthesis and characterization of thermosensitive microspheres latex. J Appl Polym Sci 96:824–828
18. Chen Y, Gautrot JE, Zhu XX (2007) Synthesis and characterization of core–shell microspheres with double thermosensitive. Langmuir 23:1047–1051
19. Sajjadi S (2007) Nanoparticle formation by monomer-starved semibatch emulsion polymerization. Langmuir 23:1018–1024
20. Ledezma R, Treviño ME, Elizalde E, Mendizábal E, Puig JE, López RG (2007) Semicontinuous heterophase polymerization under monomer starved conditions to prepare nanoparticles with narrow size distribution. J Polym Sci Part A Polym Chem 45:1463–1473
21. Aguilar J, Rabelero M, Nuño-Don Lucas SM, Mendizábal E, Martínez-Richa A, López RG, Arellano M, Puig JE (2011) Narrow-size distribution poly(methyl methacrylate) nanoparticles made by semicontinuous heterophase polymerization. J Appl Polym Sci 119:1827–1834
22. Facundo IA (2008) Nanolátices magnéticos termosensibles. Síntesis mediante polimerización en microemulsión normal. Dissertation, Centro de Investigación en Química Aplicada, México
23. Tauer K, Ramírez AG, López RG (2003) Effect of the surfactant concentration on the kinetics of oil in water microemulsion polymerization-a case study with butyl acrylate. In: Guyot A (ed) Polymer colloids (Special Edition 6). Comptes Rendus Chimie Académie des Sciences, Paris, pp 1245–1266
24. Treviño-Martínez ME, Del Angel-Vargas Y, Ramos-de Valle LF, López-Campos RG (2005) Synthesis of elastomeric nanoparticles via microemulsión polymerization. J Vinyl Addit Technol 11:132–134
25. Ramírez AG, López RG, Tauer K (2004) Studies on semibatch microemulsion polymerization of butyl acrylate: influence of the potassium peroxidisulfate concentration. Macromolecules 37:2738–2747
26. Krackeler JJ, Naidus H (1969) Particle size and molecular weight distributions of various polystyrene emulsions. J Polym Sci Part C 27:207–235
27. Smith WV, Ewart RH (1948) Kinetics of emulsion polymerization. J Chem Phys 16:592–599
28. Sajjadi S, Brooks BW (1999) Semibatch emulsion polymerization of butyl acrylate. I. Effect of monomer distribution. J Appl Polym Sci 74:3094–3110
29. Schrader D (1999) Physical constants of some important polymers. Physical constants of poly(styrene). In: Brandrup J, Immergut EH, Grulke EA (eds) Polymer handbook, 4th edn. Wiley, Hoboken, pp 91–96
30. Shields DJ, Coover HW Jr (1959) Crystalline poly(*N*-isopropylacrylamide). J Polym Sci 39:532–533